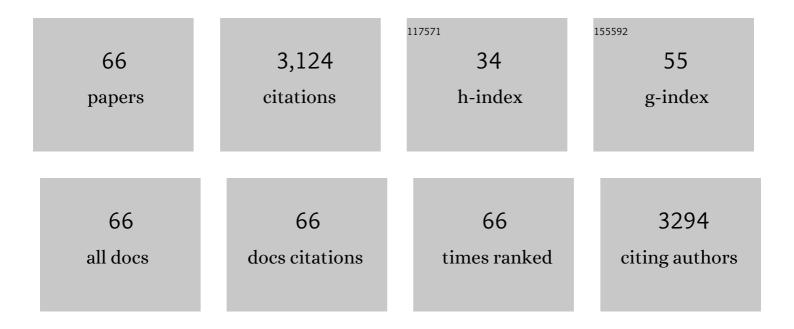
List of Publications by Year in descending order

Source: https://exaly.com/author-pdf/4204787/publications.pdf Version: 2024-02-01



FENC FL

#	Article	IF	CITATIONS
1	Synergistic effect of oxygen defect and doping engineering on S-scheme O-ZnIn2S4/TiO2-x heterojunction for effective photocatalytic hydrogen production by water reduction coupled with oxidative dehydrogenation. Chemical Engineering Journal, 2022, 430, 133125.	6.6	70
2	In-Situ Construction of 2D/2D CuCo2S4/Bi2WO6 contact heterojunction as a visible-light-driven fenton-like catalyst with highly efficient charge transfer for highly efficient degradation of tetracycline hydrochloride. Colloids and Surfaces A: Physicochemical and Engineering Aspects, 2022, 634, 127965.	2.3	14
3	In-situ anion exchange based Bi2S3/OV-Bi2MoO6 heterostructure for efficient ammonia production: A synchronized approach to strengthen NRR and OER reactions. Journal of Materials Science and Technology, 2022, 110, 152-160.	5.6	24
4	Enhancing an internal electric field by a solid solution strategy for steering bulk-charge flow and boosting photocatalytic activity of Bi24O31Cl Br10–. Chinese Journal of Catalysis, 2022, 43, 485-496.	6.9	15
5	Nanoarchitectonics of CdS/ZnSnO3 heterostructures for Z-Scheme mediated directional transfer of photo-generated charges with enhanced photocatalytic performance. International Journal of Hydrogen Energy, 2022, 47, 9566-9578.	3.8	28
6	Platinum Nanoparticle-Electrodeposited Ti ₃ C ₂ T _{<i>x</i>} MXene as a Binder-Free Electrocatalyst for Improved Hydrogen Evolution. ACS Applied Energy Materials, 2022, 5, 3092-3099.	2.5	12
7	The hierarchical layered microsphere of BiOIxBr1-x solid solution decorated with N-doped CQDs with enhanced visible light photocatalytic oxidation pollutants. Chemical Engineering Journal, 2021, 406, 127155.	6.6	45
8	Flexible ligands-dependent formation of a new column layered MOF possess 1D channel and effective separation performance for CO2. Journal of Solid State Chemistry, 2021, 294, 121896.	1.4	7
9	Synergism of carbon quantum dots and Au nanoparticles with Bi ₂ MoO ₆ for activity enhanced photocatalytic oxidative degradation of phenol. RSC Advances, 2021, 11, 28674-28684.	1.7	6
10	Giant improvement of performances of perovskite solar cells via component engineering. Journal of Colloid and Interface Science, 2021, 588, 393-400.	5.0	14
11	Novel phosphorus-doped Bi2WO6 monolayer with oxygen vacancies for superior photocatalytic water detoxication and nitrogen fixation performance. Chemical Engineering Journal, 2021, 411, 128629.	6.6	97
12	In situ fabrication of Bi2MoO6/Bi2MoO6-x homojunction photocatalyst for simultaneous photocatalytic phenol degradation and Cr(VI) reduction. Journal of Colloid and Interface Science, 2021, 599, 741-751.	5.0	80
13	Accurate guided alternating atomic layer enhance internal electric field to steering photogenerated charge separation for enhance photocatalytic activity. Applied Catalysis B: Environmental, 2021, 298, 120536.	10.8	32
14	Effective charge kinetics steering in surface plasmons coupled two-dimensional chemical Au/Bi2WO6-MoS2 heterojunction for superior photocatalytic detoxification performance. Journal of Hazardous Materials, 2020, 384, 121484.	6.5	31
15	Highly efficient visible-light-driven photo-Fenton catalytic performance over FeOOH/Bi2WO6 composite for organic pollutant degradation. Journal of Alloys and Compounds, 2020, 816, 152560.	2.8	57
16	2D/2D type-II Cu2ZnSnS4/Bi2WO6 heterojunctions to promote visible-light-driven photo-Fenton catalytic activity. Chinese Journal of Catalysis, 2020, 41, 503-513.	6.9	47
17	Synergistic introducing of oxygen vacancies and hybrid of organic semiconductor: Realizing deep structure modulation on Bi5O7I for high-efficiency photocatalytic pollutant oxidation. Applied Catalysis B: Environmental, 2020, 265, 118562.	10.8	106
18	Photocatalytic performance and mechanism insights of a S-scheme g-C ₃ N ₄ /Bi ₂ MoO ₆ heterostructure in phenol degradation and hydrogen evolution reactions under visible light. Physical Chemistry Chemical Physics, 2020, 22, 26278-26288.	1.3	55

#	Article	IF	CITATIONS
19	Desulfurization of Sulfur-Containing Compounds in Heavy Oil in the Presence of Supercritical Methanol. Energy & Fuels, 2020, 34, 2958-2968.	2.5	4
20	Highly stable and efficient perovskite solar cells produced via high-boiling point solvents and additive engineering synergistically. Science China Chemistry, 2020, 63, 818-826.	4.2	11
21	Flower-like Cu2ZnSnS4 architectures synthetize and their visible-light catalytic properties. Journal of Alloys and Compounds, 2019, 770, 424-432.	2.8	20
22	Multilayer ultrathin Ag-δ-Bi2O3 with ultrafast charge transformation for enhanced photocatalytic nitrogen fixation. Journal of Colloid and Interface Science, 2019, 533, 649-657.	5.0	45
23	Abnormal absorption onset shift of CH3NH3PbI3 film by adding PbBr2 into its precursor and its effect on photovoltaic performance. Journal of Power Sources, 2019, 437, 226914.	4.0	8
24	The Novel Z-Scheme Ternary-Component Ag/AgI/α-MoO3 Catalyst with Excellent Visible-Light Photocatalytic Oxidative Desulfurization Performance for Model Fuel. Nanomaterials, 2019, 9, 1054.	1.9	36
25	Ceramic supported attapulgite-graphene oxide composite membrane for efficient removal of heavy metal contamination. Journal of Membrane Science, 2019, 591, 117323.	4.1	66
26	Alkali-assisted synthesis of direct Z-scheme based Bi2O3/Bi2MoO6 photocatalyst for highly efficient photocatalytic degradation of phenol and hydrogen evolution reaction. Journal of Catalysis, 2019, 375, 399-409.	3.1	108
27	2D In-Plane CuS/Bi2WO6 p-n Heterostructures with Promoted Visible-Light-Driven Photo-Fenton Degradation Performance. Nanomaterials, 2019, 9, 1151.	1.9	30
28	In-Situ Construction of 2D/2D ZnIn2S4/BiOCl Heterostructure with Enhanced Photocatalytic Activity for N2 Fixation and Phenol Degradation. Catalysts, 2019, 9, 729.	1.6	48
29	Plate-to-Layer Bi2MoO6/MXene-Heterostructured Anode for Lithium-Ion Batteries. Nano-Micro Letters, 2019, 11, 81.	14.4	70
30	Synergistic effect of surface oxygen vacancies and interfacial charge transfer on Fe(III)/Bi2MoO6 for efficient photocatalysis. Applied Catalysis B: Environmental, 2019, 247, 150-162.	10.8	185
31	Magnetically recyclable Fe3O4@SiO2/Bi2WO6/Bi2S3 with visible-light-driven photocatalytic oxidative desulfurization. Materials Research Bulletin, 2019, 118, 110520.	2.7	50
32	A novel approach for high-yield solid few-layer MoS2 nanosheets with effective photocatalytic hydrogen evolution. International Journal of Hydrogen Energy, 2019, 44, 16639-16647.	3.8	12
33	Ultrafine Au nanoparticles anchored on Bi ₂ MoO ₆ with abundant surface oxygen vacancies for efficient oxygen molecule activation. Catalysis Science and Technology, 2019, 9, 3193-3202.	2.1	46
34	Fluffy honeycomb-like activated carbon from popcorn with high surface area and well-developed porosity for ultra-high efficiency adsorption of organic dyes. Bioresource Technology, 2019, 285, 121340.	4.8	116
35	Magnetically recyclable Fe3O4@SiO2/Bi2WO6â^'xF2x photocatalyst with well-designed core-shell nanostructure for the reduction of Cr(VI). Chemical Engineering Journal, 2019, 370, 1522-1533.	6.6	45
36	Chemisorption-enhanced photocatalytic nitrogen fixation via 2D ultrathin p–n heterojunction AgCl/Î'-Bi2O3 nanosheets. Journal of Catalysis, 2019, 371, 71-80.	3.1	129

#	Article	IF	CITATIONS
37	Ag/Bi2MoO6-x with enhanced visible-light-responsive photocatalytic activities via the synergistic effect of surface oxygen vacancies and surface plasmon. Applied Surface Science, 2018, 436, 536-547.	3.1	84
38	Highly selective and sensitive detection of Hg ²⁺ , Cr ₂ O ₇ ^{2â^'} , and nitrobenzene/2,4-dinitrophenol in water <i>via</i> two fluorescent Cd-CPs. New Journal of Chemistry, 2018, 42, 19844-19852.	1.4	40
39	Frontispiece: Efficient Degradation of Phenol and 4â€Nitrophenol by Surface Oxygen Vacancies and Plasmonic Silver Coâ€Modified Bi 2 MoO 6 Photocatalysts. Chemistry - A European Journal, 2018, 24, .	1.7	Ο
40	Efficient Degradation of Phenol and 4â€Nitrophenol by Surface Oxygen Vacancies and Plasmonic Silver Coâ€Modified Bi ₂ MoO ₆ Photocatalysts. Chemistry - A European Journal, 2018, 24, 18463-18478.	1.7	40
41	Organozinc Precursor-Derived Crystalline ZnO Nanoparticles: Synthesis, Characterization and Their Spectroscopic Properties. Nanomaterials, 2018, 8, 22.	1.9	23
42	A 3D supramolecular architecture based on 2,2′-oxybis(benzoic acid) and trans-1,2-bis(4-pyridyl)ethylene as ligands for Co(II). Zeitschrift Fur Naturforschung - Section B Journal of Chemical Sciences, 2017, 72, 397-401.	0.3	0
43	A two-dimensional copper(II) coordination polymer based on 2,4′-oxybis(benzoate) and 4,4′-bipyridine. Acta Crystallographica Section C, Structural Chemistry, 2017, 73, 503-507.	0.2	1
44	Effective adsorption of phenolic compound from aqueous solutions on activated semi coke. Journal of Physics and Chemistry of Solids, 2017, 102, 142-150.	1.9	42
45	Preparation of efficient Ag/AgBr/TiO2 visible light photocatalyst for destruction of MB. Journal of Materials Science: Materials in Electronics, 2017, 28, 691-696.	1.1	10
46	High-performance magnetic carbon materials in dye removal from aqueous solutions. Journal of Solid State Chemistry, 2016, 239, 265-273.	1.4	32
47	Design and construction of the sandwich-like Z-scheme multicomponent CdS/Ag/Bi ₂ MoO ₆ heterostructure with enhanced photocatalytic performance in RhB photodegradation. New Journal of Chemistry, 2016, 40, 8614-8624.	1.4	100
48	La and F co-doped Bi ₂ MoO ₆ architectures with enhanced photocatalytic performance via synergistic effect. RSC Advances, 2016, 6, 71052-71060.	1.7	51
49	Porous BiOBr/Bi ₂ MoO ₆ Heterostructures for Highly Selective Adsorption of Methylene Blue. ACS Omega, 2016, 1, 566-577.	1.6	59
50	Synthesis of nano-porous Bi 2 WO 6 hierarchical microcrystal with selective adsorption for cationic dyes. Materials Research Bulletin, 2016, 83, 387-395.	2.7	35
51	A threefold interpenetrated two-dimensional zinc(II) supramolecular architecture based on 3-nitrobenzoic acid and 4,4′-bipyridine. Acta Crystallographica Section C, Structural Chemistry, 2016, 72, 128-132.	0.2	2
52	Synthesis of Diatomite/g-C\$lt;inf\$gt;3\$lt;/inf\$gt;N\$lt;inf\$gt;4\$lt;/inf\$gt; Composite with Enhanced Visible-light-responsive Photocatalytic Activity. Wuji Cailiao Xuebao/Journal of Inorganic Materials, 2016, 31, 881.	0.6	4
53	Four new coordination polymers constructed using 2,2′-oxybis(benzoic acid) and auxiliary N-donor ligands: Syntheses, structures, magnetic behavior and DFT studies. Polyhedron, 2015, 88, 116-124.	1.0	18
54	Effective adsorption of phenol from aqueous solutions on activated semi-coke. Journal of Materials Science, 2015, 50, 4200-4208.	1.7	15

#	Article	IF	CITATIONS
55	AgBr nanoparticles decorated BiPO ₄ microrod: a novel p–n heterojunction with enhanced photocatalytic activities. RSC Advances, 2015, 5, 72830-72840.	1.7	21
56	AgBr quantum dots decorated mesoporous Bi ₂ WO ₆ architectures with enhanced photocatalytic activities for methylene blue. Journal of Materials Chemistry A, 2014, 2, 11716-11727.	5.2	211
57	Synthesis of mesoporous Bi2WO6 architectures and their gas sensitivity to ethanol. Journal of Materials Chemistry C, 2013, 1, 4153.	2.7	86
58	Monodispersed Ag nanoparticles loaded on the surface of spherical Bi2WO6 nanoarchitectures with enhanced photocatalytic activities. Journal of Materials Chemistry, 2012, 22, 4751.	6.7	194
59	Effective Adsorption of Anionic Dye, Alizarin Red S, from Aqueous Solutions on Activated Clay Modified by Iron Oxide. Industrial & Engineering Chemistry Research, 2011, 50, 9712-9717.	1.8	84
60	Stoichiometry of N-Donor Ligand Mediated Assembly in the Zn ^{II} -Hfipbb System: From a 2-Fold Interpenetrating Pillared-Network to Unique (3,4)-Connected Isomeric Nets. Crystal Growth and Design, 2011, 11, 3850-3857.	1.4	57
61	Anthraquinoneâ€2,6â€disulfonate as Versatile Ligand for the Synthesis of Hydrogenâ€Bonded Supramolecules. Zeitschrift Fur Anorganische Und Allgemeine Chemie, 2011, 637, 1432-1437.	0.6	1
62	A Novel Selfâ€assembled Dodecameric Water Cluster Stabilized by a Citrateâ€Bridged Copper(II) Compound. Chinese Journal of Chemistry, 2010, 28, 943-949.	2.6	4
63	A versatile V-shaped tetracarboxylate building block for constructing mixed-ligand Co(ii) and Mn(ii) complexes incorporating various N-donor co-ligands. CrystEngComm, 2010, 12, 1227-1237.	1.3	61
64	(4, 5)-Connected 3D Supramolecular Framework Based on 1D Tube-Shaped Coordination Armed-Chains [Mn(4,4′-bipy)(OAc) ₂] _n . Synthesis and Reactivity in Inorganic, Metal Organic, and Nano Metal Chemistry, 2009, 39, 373-378.	0.6	3
65	Two Novel 3D Hydrogenâ€bonded Architectures Constructed from Maleic Acid and Nâ€donor Ligands: Structures, Magnetic Properties and Theoretical Studies. Chinese Journal of Chemistry, 2009, 27, 273-280.	2.6	3
66	Template-Free Hydrothermal Synthesis of Novel Three-Dimensional Dendritic CdS Nanoarchitectures. Journal of Physical Chemistry C, 2009, 113, 5984-5990.	1.5	74